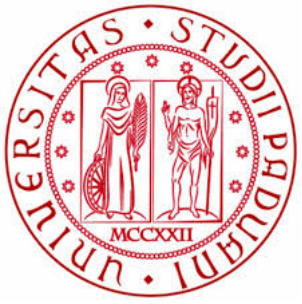

Università degli Studi di Padova

Dipartimento di Fisica e Astronomia

Corso di laurea triennale in Astronomia

Tesi di laurea

Study of techniques for determining the Mass Function of Dark Matter haloes

Laureando:
Francesco Sinigaglia
Matricola: 1121203

Relatore:
Dott. Michele Liguori

Anno Accademico 2017-2018

To Giuseppe Tormen,
passionate and cheerful professor,
expert in Cosmology and
Structure formation

CONTENTS

INTRODUCTION

The Mass Function is a very important topic in Cosmology and Large Scale Structure. This thesis examines some techniques for determining it, drawing its attention mainly on the Excursion Set theory. The aim of this work is on one hand to derive analytically the modified Press-Schechter's Mass Function, on the other hand to recover the same result from a set of simulations. In detail, the contents are subdivided into Chapters in the following way:

- Chapter 1 presents the main basic concepts of Cosmology and highlights why they are linked to the matter of this thesis;
- Chapter 2 explains how the spherical collapse of Dark Matter haloes occurs and gives some hints about the filter functions which are usually employed to smooth the density fluctuation field on a certain scale R;
- in Chapter 3 I report the analytical derivation of the Mass Function in the Press-Schechter formalism, I discuss the cloud-in-cloud problem and, in the end, I highlight that the Excursion Set theory consists in a simple but effective technique to fix the missing factor of 2 in the Press-Schechter's Mass Function;
- in Chapter 4 I carry out the aforementioned set of Excursion-Set-based simulations and try to extract the Mass Function from their results. In these simulations I choose a top-hat k-space filter function;
- Chapter 5 provides finally an explanation of how overdensity's random walks with 3 different filter functions are achieved. Furthermore, I'll compare my algorithm with that discussed previously in this Chapter.

1

BASICS OF COSMOLOGY

In this Chapter I'll provide an overview of the main basic concepts of modern Cosmology. I'll specifically go through the Friedmann equations, the Robertson-Walker metric, the main cosmological models, the cosmological parameters, the standard ΛCDM model and a brief mention of the structure formation period and of the hierarchical clustering. Moreover, I will also define the correlation function and the power spectrum. In the end I'll explain how these basics are applied to the topic this thesis is based on.

1 THE FRIEDMANN EQUATIONS AND THE COSMOLOGICAL MODELS

1.1 *The Friedmann equations and the Robertson-Walker metric*

Let us assume the validity of the Cosmological Principle and employ a set of comoving radial coordinates $\mathbf{r}$. Let then $\mathbf{x}$ indicate physical coordinates and $a(t)$ be the *scale factor*, defined as $\mathbf{r} = a(t)\,\mathbf{x}$. The scale factor $a(t)$ measures basically how physical separations between cosmic objects grows with time. The metric which is usually used to describe the geometrical properties of Universe is the *Robertson-Walker metric*, defined as

$$\mathrm{d}s^2 = \mathrm{d}t^2 - \frac{1}{c^2}\frac{a(t)^2}{a_0^2}\left[\frac{\mathrm{d}r^2}{1-kr^2} + r^2(\mathrm{d}\theta^2 + \sin^2\theta\,\mathrm{d}\phi)\right] \quad , \tag{1}$$

where r is the radial coordinate, θ and ϕ are the two Eulerian angles, k is the Universe's curvature and a_0 is the current scale factor.
The so-called Friedmann equations regulate the dynamics of Universe and are the following:

$$\left(\frac{\dot{a}}{a}\right)^2 = \frac{8\pi G}{3}\rho - \frac{kc^2}{a^2} \tag{2}$$

$$\frac{\ddot{a}}{a} = -\frac{4\pi G}{3}\left(\rho + \frac{3p}{c^2}\right) \quad , \tag{3}$$

where ρ is the matter density, G is the gravitation constant, k is the curvature and p is the matter pressure. Notice that the first equation expresses some-

how the Energy conservation, while the second one is in fact a dynamical equation. As I'll express later, an expanding Universe has an unique value of k during all its evolution and the k-value is actually what characterizes the cosmological models and makes them different from each other. Note also that, as $a(t) > 0 \, \forall t$, then the sign of $\dot{a}$ and $\ddot{a}$ depends only on the right side of the equations. Actually, since both ρ and p are positive, $\ddot{a}$ is automatically negative and therefore $a(t)$ is a concave function.

1.2 *The expanding Universe*

Before proceeding with the presentation of the main cosmological models, a brief note on the expansion of Universe is needed. The meaning of expansion is actually that distant galaxies and objects are getting further apart. The expansion of Universe becomes significant when two objects recede due to their motion not being governed by their mutual gravitational force. What the Friedmann equations express is just the 1^{st} and 2^{nd} derivatives of the scale factor, so that their solution $a(t)$ is expected to tell us whether the Universe is either contracting or expanding at a given time t.

1.3 *Cosmological models*

In this section I examine the cosmological models without the cosmological constant Λ, which will be included in the paragraph concerning the ΛCDM model. Moreover, I consider only matter dominated models, which represent roughly in a good way the evolution of Universe after the very early evolutionary phases.
The cosmological models consist in possible solutions of the Friedmann equations and differ one another for the geometry of Universe. In particular, the curvature k can be:

- $k < 0$, in case of an open Universe;
- $k > 0$, in case of a closed Universe;
- $k = 0$, in case of a flat Universe.

Sometimes the scale factor is re-scaled, so that $k = 1$ if the Universe is open and $k = -1$ if it's closed.

Let us know therefore assume $k = 0, \pm 1$. The resulting cosmological models are the following.

THE EINSTEIN-DE SITTER UNIVERSE This model corresponds with a flat Universe ($k = 0$), that is, the spacetime is a flat space. In this case the first Friedmann equation (2) loses its dependence on k and can be solved by simply separating variables, resulting in $a(t) \propto t^{2/3}$. This means that if $t \to 0$ then $a(t) \to 0$ and if $t \to \infty$ then $a(t) \to \infty$, but in a decelerated way.

THE OPEN MODEL This kind of Universe features $k = -1$ and that makes both the right-hand terms of equation (2) positive. As a result, the left-hand term $\dot{a}/a$ never becomes null nor of course negative. This fact means that the expansion is infinite and monotonic and hence $a(t) \to \pm ct$ when $t \to \infty$.

THE CLOSED MODEL In a closed Universe, at a certain $\tilde{t}$ the scale factor's derivative $\dot{a}(\tilde{t}) = 0$. As a result of this fact and of the second derivative $\ddot{a} < 0 \, \forall t$, the Universe will expand until $t = \tilde{t}$, will stop its expansion at $\tilde{t}$ and then will start to contract and will go on contracting until it performs a so-called *Big Crash*.
Figure 1 shows simultaneously the evolution of the scale factor for the three discussed models. It turns out very clearly that all these models share the feature of an initial singularity, known as *Big Bang*.

2 THE COSMOLOGICAL PARAMETERS

In order to explain the ΛCDM model, I introduce now some important cosmological parameters.
The 3 main parameters are therefore:

- the Hubble parameter $H(t)$. It is defined as $H(t) \equiv \dot{a}(t)/a(t)$ and consists in the measure of the Universe's expansion rate at the time t. The Hubble constant H_0 is none other than the Hubble parameter evaluated at the present time t_0. The galaxies in the Local Universe ($z \lesssim 1$, where z is the *redshift*) are supposed to follow a linear relation among the recession velocity and the Hubble constant. More precisely, this relation is known as *Hubble's law* and is usually expressed as

$$v = H_0 \, d \quad , \tag{4}$$

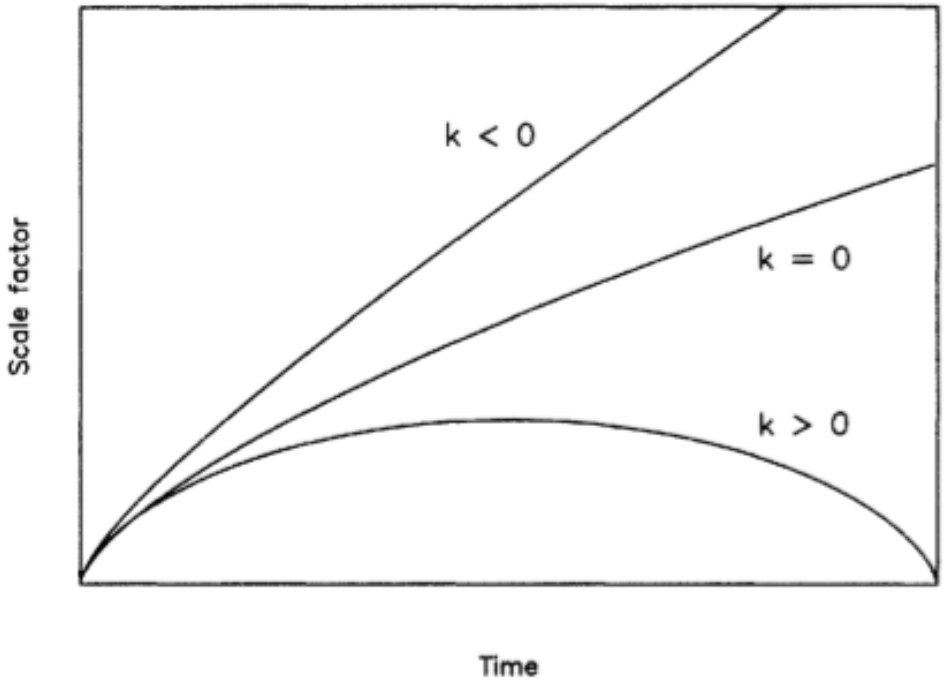

Figure 1: This plot shows the evolution of the scale factor for an Einstein-de Sitter Universe ($k = 0$), for an open Universe ($k = -1$) and for a closed Universe ($k = 1$). From Liddle A., *An Introduction to Modern Cosmology*, p.41

where v is the recession velocity, H_0 the Hubble constant and d the distance from the origin of our reference system;

- the deceleration parameter $q(t)$, defined as

$$q(t) \equiv -\frac{a(t)\,\ddot{a(t)}}{\dot{a}(t)^2} \quad . \tag{5}$$

  It is related to the scale factor's second derivative and this is why it is named after the expansion's acceleration (or equally deceleration);

- the density parameter $\Omega(t)$, which takes its name from its linear proportionality to the matter density of the Universe. It is defined as

$$\Omega(t) \equiv \frac{8\pi G}{3\,H(t)^2}\,\rho(t) \quad . \tag{6}$$

I can easily derive that $\Omega(t) = 2q(t)$ in an Universe without cosmological constant, so that actually only the determination of one out of the two latter parameters is needed. I denote the current values of the density and the acceleration parameters with Ω_0 and q_0. Regard up to this point the

density parameter as a simple matter density parameter. I'll introduce the cosmological constant Λ and the related generalized density parameter in the following paragraph.
The cosmological parameters are strictly linked to geometry of Universe. Indeed, I can derive under these circumstances the following relation linking geometry and cosmological parameters:

$$kc^2 = H_0\, a_0[\Omega(t) - 1] \quad , \tag{7}$$

where k is the Universe's curvature and a_0 the present-time scale factor. It follows quite easily from this relation that:

- if $\Omega(t) = 1$, then $k = 0$ and the Universe is flat;
- if $\Omega(t) > 1$, then $k > 0$ and the Universe is closed;
- if $\Omega(t) < 1$, the Universe is open since $k < 0$.

Hence, getting any constraints on the cosmological parameters means setting constraints also on the cosmological models.

3 THE ΛCDM MODEL

The current usual cosmological model is the so-called ΛCDM model. Such a model is named after

- on one hand, the employment of the cosmological constant Λ;
- on the other hand, the nature of the Dark Matter making up the Universe. I won't analyze more deeply this point except for saying that Dark Matter is supposed to be Cold Dark Matter (CDM, indeed), that is, is thought to be made of heavy and slow particles, e.g. WIMPs.[1]

The constant Λ came into being to explain why type Ia Supernovae of known distance appear to be further than they should be in any cosmological model, even in a model with $\rho_m = 0$, that is, a massless Universe (Milne's Universe). An agreement between data and models can be found only by setting $\Omega_0 < 0$, which doesn't appear to make sense. People found several explanations to that fact, even though basically the most popular argument is to regard such a *negative* contribution to the density parameter

1 Weakly Interactive Massive Particles

as a vacuum's energy density. I won't go through deeper details, but what actually Λ produces is a negative pressure $p_\Lambda = -\rho_\Lambda c^2$. This means that an additional expanding factor acts in the Universe and this effect must be somehow computed and taken into account. The modified Friedmann equations therefore become:

$$\left(\frac{\dot{a}}{a}\right)^2 = \frac{8\pi G}{3}\rho - \frac{kc^2}{a^2} + \frac{\Lambda}{3} \tag{8}$$

$$\frac{\ddot{a}}{a} = -\frac{4\pi G}{3}\left(\rho + \frac{3p}{c^2}\right) + \frac{\Lambda}{3} \quad , \tag{9}$$

where Λ has units $[\text{time}]^{-2}$ and represents an additional repulsive force. These equations actually come from the field equations of General Relativity and the addition of the Λ-term makes them covariant. Anyway, I can now define a proper density parameter for Λ, which is

$$\Omega_\Lambda(t) = \frac{\Lambda}{3\,H(t)} \tag{10}$$

and therefore the new overall density parameter can be expressed as

$$\Omega(t) = \Omega_m(t) + \Omega_\Lambda(t) \quad . \tag{11}$$

I'll express from now on the two present density parameters as simply Ω_m and Ω_Λ. The new geometry-parameters relation is

$$kc^2 = H_0\, a_0[\Omega_m(t) + \Omega_\Lambda(t) - 1] \quad , \tag{12}$$

where the flatness of Universe now requires $\Omega_m(t) + \Omega_\Lambda(t) = 1$. Actually, thanks to COBE's, WMAP's and Planck's data, we managed to fix the overall current density parameter $\Omega_0 \sim 1$ with a very small error, so that we can regard the Universe as flat and anyway, if not perfectly flat, to be not much closed or open.

4 STRUCTURE FORMATION AND HIERARCHICAL CLUSTERING

I'll complete this introductory Chapter by presenting some general basics about Structure formation. More specific notions will be provided in the following Chapters.

Structure formation begun to occur after the so-called *Recombination epoch*, at redshift $z \sim 1080$, that is, almost 389000 years after the Big Bang. At that era, the matter decoupled from radiation and the Universe became transparent, as it is known nowadays. The formation of structures takes place qualitatively in the following way. After an initial time, say Recombination, the temperature of Universe started to decrease rapidly as so did until *Re-ionization* took place. The key point is supposing that at the Recombination there were some irregularities in the matter distribution, so that density wasn't a homogeneous field at all. This is not surprising. Even though we usually employ the Cosmological Principle with regard to the whole Universe, it turns out to be a good assumption only on scales larger than hundreds Megaparsecs, say 500 Mpc. It is easily verifiable, by for instance observing optical galaxies, that on scales smaller than $100 - 500$ Mpc the Universe is anything but isotropic and homogeneous. Anyway, what happens is that the overdense regions exert a greater gravitational force to their surroundings and tend to draw material in. These regions become therefore denser and denser, making the forming proto-structures more and more massive and gradually shaped as time goes by. I discuss the details of the collapse of haloes in the following Chapter. Once the smallest structures have formed, they tend to cluster and form larger structures consisting in group of the former, due to their mutual gravitational attraction. This phenomenon is known as *hierarchical clustering*. The resulting scenario is an Universe made of gradually larger and larger structures, as a result of the clustering of smaller substructures.

5 THE CORRELATION FUNCTION AND THE POWER SPECTRUM

Let ρ be the matter density of a given region characterized by some deviations from the homogeneity of the density field, ρ_b be the matter density of the background. I define the contrast density field evaluated at the point of coordinates $\mathbf{x}$ as

$$\delta(\mathbf{x}) = \frac{\rho - \rho_b}{\rho_b} \quad . \tag{13}$$

I then define the so-called *correlation function* as

$$\xi(r) \equiv \langle \delta(\mathbf{x}) \,|\, \delta(\mathbf{x}+\mathbf{r}) \rangle \quad , \tag{14}$$

where r is the magnitude of the vector $\mathbf{r}$. The meaning of the correlation function is basically estimating how likely is finding the same contrast density at the points $\mathbf{x}$ and $\mathbf{x}+\mathbf{r}$. In other words, given a cosmic structure at the point $\mathbf{x}$, it provides the probability of finding another structure at a radial distance r. The correlation function can be written in a more extended form by simply expressing the scalar product in its integral form

$$\xi(r) = \frac{1}{(2\pi)^6} \int \mathrm{d}^3k \int \mathrm{d}^3k' \ \langle \hat{\delta}(k) \,|\, \hat{\delta}(k') \rangle \ e^{i\mathbf{k}\cdot(\mathbf{x}+\mathbf{r})} \, e^{i\mathbf{k'}\cdot\mathbf{x}} \quad . \tag{15}$$

I define the *power spectrum* $P(k)$ by linking it to the k-space perturbation with the relation

$$\langle \hat{\delta}(k) \,|\, \hat{\delta}(k') \rangle \equiv (2\pi)^3 \, P(k) \, \delta_D^{(3)} \, (\mathbf{k}+\mathbf{k'}) \quad , \tag{16}$$

where $\delta_D^{(3)}$ is a 3-dimensional Dirac's delta. By substituting this relation in equation (15), by making the Dirac's delta acting and by computing the integral in the variable k' getting 1 as a result, I find the relation

$$\xi(r) = \frac{1}{(2\pi)^3} \int \mathrm{d}^3k \, P(k) \, e^{i\mathbf{k'}\cdot\mathbf{x}} \quad . \tag{17}$$

This important relation shows clearly that the power spectrum is the Fourier transform of the correlation function. This result is also known as *Wiener-Khintchine* theorem. As the power spectrum $P(K) \propto |\hat{\delta}(\mathbf{k})|^2$, it is proportional to the amplitude of a plane wave whose wavenumber is k. This means that the power spectrum tells us how much a density fluctuation on a scale k contributes to form the generic contrast density $\delta(\mathbf{x})$. $P(k)$ represents therefore the power of a fluctuation on the scale k.

6 APPLICATION TO THIS THESIS

This thesis aims to go through the main techniques for determining the Mass Function of Dark Matter haloes. Hence, it appears quite obvious that the brief introduction to Structure formation I carried out in the previous paragraph was needed. Then, in this thesis I'll mention again the density parameter Ω_m, as the Mass Function can be used to derive some constraints on Ω_m. As far as the cosmological models are concerned, a collapsing halo behaves like a closed Universe, while the background keeps on expanding,

say in flat-Universe-like way. This is why I need also an overview of the cosmological models. In the end, in the last Chapter I'll analyse a technique considering the power spectrum of density perturbations, so an introduction to that topic is useful too.

2

THE SPHERICAL COLLAPSE

This Chapter provides a brief but useful explanation about how the spherical collapse occurs. Even though the actual formation of Dark Matter haloes takes place in an ellipsoidal collapse, the spherical model can be regarded as a good approximation of the real collapse.

1 THE GROWTH OF PERTURBATIONS AND THE COLLAPSE

Let ρ be the local matter density and ρ_b be the background density. A collapse happens basically when the matter density ρ locally suffers a perturbation, that is, when an overdensity $\delta = (\rho - \rho_b)/\rho_b > 0$ comes into being.
Let us now consider a region in which a top-hat overdensity δ occurs and employ these two following hypothesis:

- the initial peculiar velocity of the matter in this region is null;
- different mass shells don't cross each other during the evolution of the region.

What qualitatively occurs is that, during the expansion, the evolution of the background and the overdense region is well-modelled by the Friedmann equations respectively for a flat Universe without Λ and a closed Universe. Hence, both the background and the perturbation expand, but the latter expands more slowly. This fact makes it clear that the contrast density grows in magnitude more and more. The expansion of the overdense region goes on until δ reaches a critical value, then it stops its expansion, detaches from the background and starts contracting, performing a collapse. Actually, even though the collapse is regarded to be the point at which the density diverges, a halo virializes before really completely collapsing.

2 THE MODEL

2.1 *The background*

Let us now begin with the background and consider the first Friedmann equation, setting $k = 0$ as for a flat Universe and $\rho = \rho_b$:

$$\left(\frac{\dot{a}_b(t)}{a_b(t)}\right)^2 = \frac{8\pi G}{3}\rho_b \quad , \tag{18}$$

where $a_b(t)$ is the background's scale factor. As in a flat Universe $a(t) \propto t^{2/3}$, then also $\dot{a}(t) \propto t^{2/3}$. By substituting these relations in the Friedmann equation, it turns out that

$$\rho_b = \frac{1}{6\pi\, G\, t^2} \quad . \tag{19}$$

2.2 *The perturbation*

Let us now start by introducing a new variable η, which is related to the variable t by the differential relation

$$\mathrm{d}\eta = \mathrm{d}t\, \frac{c}{a(t)} \quad , \tag{20}$$

where c is the light speed. By derivating $a(t)$ in respect with η instead of t, by substituting it in the Friedmann equation and by multiplying both sides by $a(t)^2$), I get

$$\left(\frac{\mathrm{d}a}{\mathrm{d}\eta}\right)^2 = \left[\frac{a(t)}{c}\right]^2 \left[\frac{8\pi\, G}{3}\rho\, a^2 \,-\, kc^2\right] = \frac{8\pi\, G}{3}\rho\, a(t)^4 \,-\, ka(t)^2 \quad . \tag{21}$$

Thanks to the hypothesis of *shell crossing* not occurring, the conservation of mass within each mass shell is guaranteed and this allows me to express ρ as:

$$\rho(t) = \rho_0 \frac{a(t)}{a_0} \quad , \tag{22}$$

where ρ_0 and a_0 represent respectively the matter density and the scale factor at the present time (or at any arbitrary time). By substituting it in the Friedmann equation I get

$$\left(\frac{\mathrm{d}a}{\mathrm{d}\eta}\right)^2 = \frac{8\pi G}{3c^2}\rho_0 a_0^3 a(t) - k a(t)^2 \quad . \tag{23}$$

Introduce now $\tilde{a} = 4\pi G\rho_0 a_0^3/3c^2$, set $x = a/\tilde{a}$ and fix $k = 1$ as in a closed Universe. Then the Friedmann equation becomes

$$\left(\frac{\mathrm{d}x}{\mathrm{d}\eta}\right)^2 = 2x - x^2 \quad , \tag{24}$$

and allows me to achieve the following solution:

$$x = \frac{a(t)}{\tilde{a}} = 1 - \cos\eta \quad . \tag{25}$$

Now, in the first place I can find a parametrization $t(\eta)$ just by multiplying and dividing by $\tilde{a}$, by substituting the solution $x = 1 - \cos\eta$ in equation (20) and by solving the integral:

$$t(\eta) = \int_0^\eta \mathrm{d}\eta' \frac{a(\eta')}{c} = \frac{\tilde{a}}{c}\int_0^\eta \mathrm{d}\eta' (1 - \cos\eta') = \frac{\tilde{a}}{c}(\eta - \sin\eta) \quad . \tag{26}$$

In the second place, in this re-parametrization the function $a(\eta)$ represents a cycloid and turns out to be useful to study the evolution of the perturbation. Indeed, as already reported above, the perturbed region expands more and more slowly if compared to the background and this makes the contrast density δ growing more and more. The point at which the perturbation stops expanding and starts its collapse is usually known as *turn-around* and takes place at $\eta = \pi$ in this new parametrization, while the collapse occurs at $\eta = 2\pi$. It turns out easily by setting $\eta = \pi$ also that the scale factor at the turn-around is $a_{TA} = a(\pi) = 2\tilde{a}$.
The point is now trying to compute which is the threshold value of δ that makes a halo collapsing if overtaken. I'll proceed deriving the contrast density value at the turn-around and at the collapse both in the linear and non-linear theory. Note first of all that the overdensity can be written as

$$1 + \delta(\eta) = \frac{\rho_m(\eta)}{\rho_b(\eta)} = \frac{4}{3}\rho_0 a_0^3 \frac{G}{\tilde{a}c^2}\frac{9(\eta - \sin\eta)^2}{2(1 - \cos\eta)^3} = \frac{9(\eta - \sin\eta)^2}{2(1 - \cos\eta)^3} \tag{27}$$

The non-linear values follow simply by setting:

- $\eta = \pi$ at the turn-around, so that

$$1 + \delta(\pi) = 1 + \delta_{TA} = \frac{9}{2}\frac{\pi}{8} = 5.55 \quad ; \tag{28}$$

- $\eta \to 2\pi$ when the halo collapses and at that moment the contrast density $\delta \to \infty$.

In order to derive the aforementioned values in the linear theory, let us consider small values of η, i.e. $\eta \ll 1$. In this approximation the linear theory can be applied and I can therefore expand the two terms $(\eta - \sin\eta)^2$ and $(1 - \cos\eta)^3$ in a Taylor series. The two expansions I use are therefore:

- $(\eta - \sin\eta)^2 \sim \left[\eta - \left(\eta - \frac{\eta^3}{3!} + \frac{\eta^5}{5!} + \dots\right)\right]^2$;
- $(1 - \cos\eta)^3 \sim \left[1 - \left(1 - \frac{\eta^2}{2!} + \frac{\eta^4}{4!} + \dots\right)\right]^3$.

By substituting them in equation (27) I get

$$1 + \delta(\eta) \sim \frac{9\left[\eta - \left(\eta - \frac{\eta^3}{3!} + \frac{\eta^5}{5!} + \dots\right)\right]^2}{2\left[1 - \left(1 - \frac{\eta^2}{2!} + \frac{\eta^4}{4!} + \dots\right)\right]^3} = \frac{9}{2}\frac{\left(\frac{\eta^3}{6} - \frac{\eta^5}{120}\right)^2}{\left(\frac{\eta^2}{2} - \frac{\eta^4}{24}\right)^3} \simeq \frac{9}{2}\frac{\frac{\eta^6}{36}\left(1 - \frac{\eta^2}{10}\right)}{\frac{\eta^6}{8}\left(1 - \frac{\eta^2}{4}\right)} \quad . \tag{29}$$

In case of $x \ll 1$ I can also make use of the Taylor expansion $(1 - x)^{-1} \sim 1 + x$, so that I derive:

$$1 + \delta(\eta) \sim \frac{9}{2}\left[\frac{2}{9}\left(1 - \frac{\eta^2}{10}\right)\left(1 + \frac{\eta^2}{4}\right)\right] = \frac{9}{2}\left(\frac{2}{9} + \eta^2\left(\frac{1}{18} - \frac{1}{45}\right)\right) \quad . \tag{30}$$

Since what I'm interested in is the overdensity $\delta(\eta)$, by subtracting both sides by a factor of 1 I manage to derive

$$\delta(\eta) \sim \frac{3}{20}\eta^2 \quad . \tag{31}$$

I must now express η again in term of the starting variable t. This can be easily done by considering that for small values of η the integral in equation (26) corresponds to the integrand function evaluated in η. Furthermore, I can again make use of Taylor expansions, so that

$$t(\eta) \sim \frac{\tilde{a}}{c}(\eta - \sin\eta) \sim \frac{\tilde{a}}{c}\frac{\eta^3}{6} \quad . \tag{32}$$

Let us now indeed derive $\eta(t)$ by inverting equation (32):

$$\eta(t) = \left(\frac{6c}{\tilde{a}}\, t\right)^{1/3} \quad . \tag{33}$$

In the end by substituting the expression of $\eta(t)$ I have just derived in equation (31) I get

$$\delta(t) = \frac{3}{20}\left(\frac{6c}{\tilde{a}}\, t\right)^{2/3} \quad . \tag{34}$$

The δ-values I compute using the linear theory are therefore:

- $\delta_{lin,TA} = \delta(t = \frac{\tilde{a}}{c}\pi) = \frac{3}{20}(6\pi)^{2/3} = 1.06$, at the turn-around;
- $\delta_{lin,coll} = \delta(t = \frac{\tilde{a}}{c}2\pi) = \frac{3}{20}(12\pi)^{2/3} = 1.686$, for the collapse.

3 THE VIRIALIZATION

Actually, as I anticipated above a halo doesn't collapse making its matter density diverging but virializes and stabilises, while its radius becomes half of the turn-around radius. This happens because the radial velocities become partially tangential during the collapse due to the gravitational interactions between particles. Moreover, when it happens the δ-value ~ 178.

Let us now derive these results by applying the Virial Theorem to both the turn-around and the virialization. Remember also that, as gravity is the only force acting on the system, the energy is conserved: $E = U + T =$ constant. At the turn-around, $T_{TA} = 0$, so that

$$E_{TA} = U_{TA} = -\alpha\frac{GM}{R_{TA}} \quad , \tag{35}$$

where the parameter α takes into account the mass distribution and hence also possible variations of the density profile. When the halo virializes the Virial Theorem tells us that

$$2T_{vir} + U_{vir} = 0 \Longleftrightarrow T_{vir} = -\frac{U_{vir}}{2} \quad . \tag{36}$$

By substituting this result in the energy conservation and by supposing the density profile and therefore the parameter α to remain constant, it turns out that

$$E_{vir} = U_{vir} + T_{vir} = \frac{U_{vir}}{2} = -\alpha \frac{GM}{2R_{vir}} = -\alpha \frac{GM}{R_{TA}} \quad . \tag{37}$$

By simply comparing the denominators I easily get $R_{vir} = R_{TA}/2$. Let us now compute the value of δ in the non-linear theory. I'll start by making the following considerations:

- in a flat Universe $a(t) \propto t^{2/3}$;
- as $\rho \propto a(t)^{-3}$, then $\rho \propto t^{-2}$. Furthermore, $t_{vir} = 2t_{TA}$. Due to these facts, $\frac{\rho_{b,TA}}{\rho_{b,vir}} = \frac{t_{vir}^2}{t_{TA}^2} = 4$;
- as $R_{TA} = 2R_{vir}$, then $\frac{\rho_{vir}}{\rho_{TA}} = 8$;
- remember that $\frac{\rho_{TA}}{\rho_{b,TA}} = 5.55$.

The point is now computing $1 + \delta_{vir} = \rho_{vir}/\rho_{b,vir}$. Let us multiply and divide both sides by ρ_{TA} and $\rho_{b,TA}$. What I get is

$$1 + \delta_{vir} = \frac{\rho_{vir}}{\rho_{b,vir}} = \frac{\rho_{vir}}{\rho_{TA}} \frac{\rho_{b,TA}}{\rho_{b,vir}} \frac{\rho_{TA}}{\rho_{b,TA}} = 8 \cdot 4 \cdot 5.55 \simeq 178 \quad , \tag{38}$$

which turns out be an exact solution in the considered case of the spherical collapse. Hence, in an Einstein-de Sitter Universe with $\Omega_m = 1$, the virializing non-linear overdensity is $\delta = 178$. In a general framework, an Universe without cosmological constant Λ features $1 + \delta_{vir} = 178\,\Omega_m^{-0.7}$, that is, a weak dependence on the cosmological model. In the end, the ΛCDM model would have a higher δ_{vir}-value because the background expands more rapidly and then its density results to decrease more quickly.

4 THE FILTER FUNCTIONS

This ending section provides a brief introduction to the filter functions I'm going to use in the following Chapters.
A *filter* function (or equally *window* function) consists in a function that somehow weights the matter density in an effective way for the considered application. It is therefore important because a contrast density δ on a particular scale R can be properly well defined only with the aid of such

a window function. Let indeed $W(x, R)$ be a generic filter and let $\delta(\mathbf{x})$ be the overdensity located at a point of comoving coordinates $\mathbf{x}$. Let x be the absolute value of the vector $\mathbf{x}$. Note that the field δ doesn't provide any information about the overdensity's scale R. Hence, this information can be obtained by computing the integral

$$\delta(\mathbf{x}, R) = \int \mathrm{d}^3x' \, W(|\mathbf{x'} - \mathbf{x}|, R) \, \delta(\mathbf{x'}) \quad . \tag{39}$$

In other words, the field $\delta(\mathbf{x}, R)$ can be obtained by convolving the contrast density field with the window function.
Equation (39) tells us also that the filter function has dimensions of inverse volume because the field $\delta(\mathbf{x})$ is dimensionless and so must be the field $\delta(\mathbf{x}, R)$. If we then consider the normalized function $W'(x, R)$, it is possible to associate to W' a volume V_W. The volume V_W can be derived by computing the integral

$$V_W = \int \mathrm{d}^3x \, W'(x) \quad . \tag{40}$$

One can think about the smoothed density field as a kind of average of the density fluctuation in a region of volume $V_W \sim R^3$, where R is the scale on which the filter acts. Moreover, as in the real space the smoothed density field $\delta(\mathbf{x}, R)$ is represented by a convolution, in the Fourier space it can be computed with a simple product. Indeed, let $W(k, R)$ and $\delta(\mathbf{k})$ be respectively the window and contrast density in the k-space. Let also k be the absolute value of the vector $\mathbf{k}$. Then I can compute the Fourier transform of the smoothed density as

$$\delta(\mathbf{k}, R) = W(k, R) \, \delta(\mathbf{k}) \quad . \tag{41}$$

The choice of the filter also establishes a relation between the smoothing scale R and the mass M. The most popular choices have been over the years the following filters:

- a top-hat window in the real space: the function is defined as

$$W(x, R) = \begin{cases} \frac{3}{4\pi R^3} & \text{if } x \leq R \\ 0 & \text{if } x > R \end{cases} \tag{42}$$

This filter has a well-defined volume which is simply the volume of a sphere of radius R. In this way the halo's mass turns out to be $M = \frac{4}{3}\pi\rho_M R^3$;

- a top-hat filter in the k-space, defined as

$$W(k, R) = \begin{cases} 1 & \text{if } k \leq 1/R \\ 0 & \text{if } k > 1/R \end{cases} \quad . \tag{43}$$

The problem with this function is that it doesn't have a well-defined volume V_W in the real space;

- a Gaussian window in the real space, defined as

$$W(x, R) = \frac{1}{(2\pi)^{3/2} R^3} e^{-\frac{x^2}{2R^2}} \quad . \tag{44}$$

Its volume can be computed as $V_W = (2\pi)^{3/2} R^3$ and therefore the halo's mass will be $M = (2\pi)^{3/2}\rho_M R^3$.

In the next Chapter I'll make use of the top-hat filters both in the real and in the k-space.

3

MASS FUNCTION AND EXCURSION SET THEORY

This chapter aims to introduce the concept of Mass Function of Dark Matter haloes, the Press-Schechter formalism and the application of the Excursion Set theory in order to fix the missing factor 2 in the Press-Schechter derivation. In all this Chapter I will of course make use of comoving coordinates. The reference this Chapter is based on is Zentner(2007).

1 MASS FUNCTION

According to the Cosmological Principle, let us consider an isotropic and homogeneous Universe, let M be the mass of a general virialized objects and n be the number density of collapsed objects. The Mass Function is defined as $\Phi(M) = \mathrm{d}n/\mathrm{d}M$ and is useful because $\Phi(M)\,\mathrm{d}M$ provides the number density of virialized objects whose mass lays between M and $M + \mathrm{d}M$. In other words, it expresses the probability for an infinitesimal element of fluid to belong to an object of mass $m \in [M, M + dM]$.
Since Dark Matter gives a contribute to the overall density of matter which is roughly 6 times that of baryonic matter $\rho_{m,bar}$, I'm interested in studying the Mass Function of Dark Matter haloes. The Mass Function is a very useful and important topic in Cosmology as f.i. it allows us to:

- study the mass spectrum of cosmological structures and understand which percentage of haloes belongs to a certain mass interval;
- try to get some constraints on the cosmological parameters. If we indeed consider the Ω_m parameter, as defined in Chapter 1, we can derive a lower limit[1] for the density of matter ρ_M by computing the following integral:

$$\rho_m = \int_0^\infty \Phi(M)\, M\, \mathrm{d}M \tag{45}$$

  and by dividing ρ_m by the *ad-hoc* defined critical density ρ_c I would get a value for Ω_m.

1 In this way, mass which doesn't belong to virialized objects hasn't been taken into account

- find a good analytical form for the Luminosity Function of galaxies, which is somehow related to the Mass Function and is well-fitted by a Press-Schechter-type function.[2]

2 THE PRESS-SCHECHTER FORMALISM

W.H. Press and P. Schechter derived in Press&Schechter(1974) an analytical form for the Mass Function. Let R be the radial coordinate of a halo. In this work they assumed that a halo collapses on some small scale R when the linear density contrast field exceeds a certain threshold δ_c, which depends weakly on the employed cosmological model. The threshold value δ_c can be computed in the linear theory of spherical collapse and turns out to be $\delta_c = 1.686$. Moreover, in their theory they assumed that the smoothed density contrast on the mentioned scale R doesn't affect the behaviour of regions on scales larger than R. In order to do that, it is necessary to choose a proper filter, which must be function of the smoothing scale R, for the density contrast. In order to be consistent with the spherical collapse theory I'll choose in this paragraph a real top-hat filter.
The analytical derivation is as follows. Let us assume that the density fluctuation is a Gaussian random variable: the density fluctuation field $\delta(\mathbf{x}, R)$ will therefore be a Gaussian random field as well because it consists in a sum of Gaussian random variables. Let $\sigma^2(r)$ be the mass variance of the latter. Then the probability of $\delta(\mathbf{x}, R)$ laying in a density contrast interval $[\delta,\, \delta + \mathrm{d}\delta]$ can be expressed as:

$$P(\delta,\, R)\,\mathrm{d}\delta = \frac{1}{\sqrt{2\pi\,\sigma^2(R)}} e^{-\frac{\delta^2}{2\sigma^2(R)}}\,\mathrm{d}\delta \quad , \tag{46}$$

according to the choice of a Gaussian field. Since the smoothing scale R corresponds to a mass M of the halo as reported above, we can make use of the mass coordinate instead of the radial one. Then the probability of having a region of mass M with a density fluctuation above δ_c follows by integrating $P(\delta,\, R)\mathrm{d}\delta$ over all the density contrasts, from the threshold δ_c to infinite:

$$F(M) = \int_{\delta_c}^{\infty} P(\delta,\, R)\mathrm{d}\delta = \frac{1}{2}\mathrm{erfc}\left(\frac{\delta_c}{\sqrt{2}\,\sigma(M)}\right) \quad , \tag{47}$$

2 Even though haloes are thought to be sites of galaxy formation, the connection between the Mass Functions of galaxies and haloes isn't so clear yet.

where $\mathrm{erfc}(x)$ is thus the complementary error function. Note that I expressed again $\sigma(M)$ as a function of M instead of R and that the ratio $\delta_c/\sigma(M)$ represents the height of the threshold in units of the standard deviation of the δ field. This means that each epoch is characterized by a certain typical scale $M^\star$ which collapses when the mass variance $\sigma(M^\star) = \delta_c$, so that $\delta_c/\sigma(M\star) = 1$.
Under these conditions, the number of virialized objects with masses in $[M,\, M + \mathrm{d}M]$ is given by:

$$\Phi(M)\,\mathrm{d}M = \frac{\mathrm{d}n}{\mathrm{d}M}\,\mathrm{d}M = \frac{\rho_M}{M}\left|\frac{\mathrm{d}F(M)}{\mathrm{d}M}\right|\mathrm{d}M \quad , \tag{48}$$

where the factor ρ_M/M multiplies the remaining part by the number density of particles of fluid at the scale M. In such a way, the normalization of $F(M)$ is lost and the function $\Phi(M)\,\mathrm{d}M$ gives the number density of haloes at the considered scale.
Using further calculations it is possible to derive the final form of the Press-Schechter Mass Function:

$$\Phi(M)\,\mathrm{d}M = \frac{\mathrm{d}n}{\mathrm{d}M}\,\mathrm{d}M = \frac{\rho_M}{M}\frac{1}{\sqrt{2\pi\,\sigma^2(M)}}\,2\,\frac{\delta_c}{2\,\sigma(M)}\frac{\mathrm{d}\left(\frac{\delta_c^2}{\sigma(M)}\right)}{\mathrm{d}M}\,e^{-\frac{\delta_c^2}{2\sigma^2(M)}}\,\mathrm{d}M \tag{49}$$

by multiplying and dividing by M in order to get the logarithmic derivative and by setting $\nu = \delta_c/\sigma(M)$

$$\Phi(M)\,\mathrm{d}M = \frac{\mathrm{d}n}{\mathrm{d}M}\,\mathrm{d}M = \frac{\rho_M}{M^2}\frac{1}{\sqrt{2\pi}}\,\nu\frac{\mathrm{d}\ln\nu}{\mathrm{d}\ln M}\,e^{-\frac{\nu^2}{2}}\,\mathrm{d}M \quad . \tag{50}$$

By analizing its features it turns out that:

- the mass function resembles a power law $\mathrm{d}n/\mathrm{d}M \propto M^{-2}$ at small scales $M \ll M^\star$;
- it shows a *cut-off* when $M \gtrsim M^\star$, as the exponential factor overwhelms the power-law one in that case.

3 THE CLOUD-IN-CLOUD PROBLEM

The above defined mass function features a serious problem. Indeed, by definition $\mathrm{erfc}(0) = 1$ and this results in $F(M) = 1/2$ in the Press-Schechter formalism if $\nu = 0$. Since considering $\nu = 0$ (which is the same of $\delta = 0$)

implies considering all the structures that have formed due to a null density contrast, that is, considering all mass in virialized objects, then equation (47) states that only half of the mass density in the universe is part of virialized haloes.

This problem is due to not taking into account that if the density fluctuation $\delta(\mathbf{x}, M)$ is above the threshold at a certain scale M, it could be below the threshold δ_c at a smaller scale $M^+ < M$. What just expressed is usually known as the *cloud-in-cloud* problem. Press and Schechter were aware of such an issue and tried to fix their Mass Function by stating that, if the problem at a certain scale was having neglected underdense regions as discussed above, then such underdense regions would collapse onto overdense regions on a larger scale. Due to this heuristic argument, Press and Schechter simply multiplied their Mass Function by a factor of 2. On one hand, it turns to be clear they did it in order to take into account that more mass should be contained in bound haloes than how much was predicted by their derivation. This is why in a way of course this additional factor of 2 makes sense. On the other hand, the hypothesis this argument should lead exactly to a factor of 2 is at least debatable.

4 EXCURSION SET THEORY

The Excursion Set Theory is a semi-analytical technique consisting basically in a set of rules used for assigning mass elements to haloes of various sizes. In order to overcome the cloud-in-cloud problem, the point is trying to compute the probability that the first up-crossing of the threshold δ_c occurs on a scale R.

Let's start by fixing the coordinates $\mathbf{x}$, so that we can consider $\delta(R)$ has only an explicit dependence on the scale R. Since the standard deviation $\sigma(R)$ decreases monotonically with decreasing scale R, according to the form of the power spectrum $P(k)$, let $S = \sigma^2(R)$ be the new parameter which I'll use to denote the smoothing scale from now on. The problem becomes therefore trying to compute the probability for the first up-crossing to occur in an interval $[S, S + dS]$.

Let's start by considering a certain large scale R, that is, a small S, at which $\delta(S_1) \equiv \delta_1 < \delta_c$ and consider an increment $\Delta S = S_2 - S_1 > 0$. After this increment, there will be a certain probability of the contrast density exceeding the threshold. However, in a general framework, the exceeding-δ_c

probability depends not only on the size of the step ΔS, but also on the value of the density field on other scales, making the problem rather complicated. An important and nice case is when the filter function used to define the density fluctuation δ is a top-hat one in the $k-$space. In that case, the probability of the contrast density suffering a variation $\Delta\delta$ during the step ΔS is Gaussian with zero mean and variance $\sigma = \Delta S$, regardless of the starting scale S_1. Hence, a top-hat filter in the k-space allows the $(\Delta\delta, \Delta S)$ steps to be independent on each other. Note that this choice isn't the most general at all: one could in principle choose other windows filter functions, even though calculations would be more complicated because it would be necessary to find the proper correlation between the steps. It is common to refer to the function $\delta(S)$ as a trajectory performing a Brownian random walk.

Let us now derive the Mass Function under the above employed conditions. The probability of a transition $\Delta\delta = \delta_2 - \delta_1$, $\delta_2 > \delta_1$ is

$$P(\delta_2, S_2)\mathrm{d}\delta_2 = G(\Delta\delta, \Delta S)\,\mathrm{d}(\Delta\delta) \quad \text{, where} \tag{51}$$

$$G(\Delta\delta, \Delta S)\,\mathrm{d}(\Delta\delta) = \frac{1}{\sqrt{2\pi\,\Delta S}}\, e^{-\frac{(\Delta\delta)^2}{2\Delta S}}\,\mathrm{d}(\Delta\delta) \quad . \tag{52}$$

is the Gaussian transition probability.

Consider now the probability distribution $P(\delta, S + \Delta S)$ on a subsequent S step (we're moving towards larger S, that is, a smaller scale R): it can be related to the probability distribution $P(\delta, S)$ by a convolution with the Gaussian distribution $G(\Delta\delta, \Delta S)$

$$P(\delta, S + \Delta S) = \int \mathrm{d}\delta\, G(\Delta\delta, \Delta S)\, P(\delta - \Delta\delta, S) \quad . \tag{53}$$

Then, by using a Taylor expansion up to the 2^{nd} order of the previous relation for small transitions and by integrating each term, I get:

$$\frac{\partial P}{\partial S} = \lim_{\Delta S \to 0} \left(\frac{\overline{(\Delta\delta)^2}}{2\,\Delta S} \frac{\partial^2 P}{\partial \delta^2} - \frac{\overline{\Delta\delta}}{\Delta S} \frac{\partial P}{\partial \delta} \right) \quad , \tag{54}$$

where the line over $\Delta\delta$ indicates an average.

Use now the fact that, if we assume a top-hat filter in the k-space, the

transition probability is Gaussian, so that $\overline{\Delta\delta} = 0$, and $\Delta S = \sigma^2 = \overline{(\Delta\delta)^2}$. By doing that, we get the following diffusion equation:

$$\frac{\partial P}{\partial S} = \frac{1}{2}\frac{\partial^2 P}{\partial \delta^2} \tag{55}$$

The aim of this procedure is deriving the Mass Function by considering all the trajectories that has overtaken the threshold δ_c before or just at a certain scale S. However, this way would require proper boundary conditions that aren't immediate, so that it appears more simple to solve the equation by computing the probability of the trajectories not to exceed δ_c prior to the scale S and then deriving the quantity we are interested in by subtraction. The first boundary condition is that $P(\delta, S)$ must be finite when $\delta \to -\infty$, which will turn out to be useful later. The second but most important boundary condition for a $\delta(S)$ random walk never piercing the threshold is $P(\delta_c, S) = 0$, since the probability of crossing the barrier up to the scale S is null. Let now γ a new shifted variable $\Delta\delta = \delta_c - \delta = \gamma$, so that $P(\gamma, S)$ denotes the probability of passing the threshold at the scale S. The boundary condition becomes therefore $P(0, S) = 0$. I will now solve equation (55) in the Fourier-space. Let $\hat{P}$ be the Fourier transform of the probability distribution:

$$\hat{P}(k) = \int \mathrm{d}\gamma\, P(\gamma, S)\, e^{-i\omega\gamma} \quad \text{, where} \quad \omega = 2\pi k \tag{56}$$

Consider now the relation for the Fourier transform:

$$f(x) = \frac{\mathrm{d}g(x)}{\mathrm{d}x} \iff \hat{f(x)} = i2\pi k\, g(x) \quad . \tag{57}$$

By using that, equation (55) becomes

$$\frac{\partial \hat{P}}{\partial S} = -\frac{\omega^2}{2}\hat{P} \quad , \tag{58}$$

whose solution can be obtained by separating variables and integrating. It turns out to be

$$\hat{P}(\omega, S) = c(\omega)\, e^{-\frac{\omega^2}{2}S} \quad , \tag{59}$$

where $c(\omega)$ arises from the integration and must be somehow determined. For this purpose, I'll make use of the boundary condition $P(\gamma = 0, S) = 0$, which is responsible for the function $c(\omega)$ being odd. This means that

$c(\omega)\, e^{-\frac{\omega^2}{2}S}$ is still an odd function and its Fourier transform can be done by considering only the imaginary part:

$$P(\gamma, S) = \int_0^\infty c(\omega)\, \sin(\omega\gamma)\, e^{-\frac{\omega^2}{2}S}\, \mathrm{d}\omega \quad . \tag{60}$$

Then, in order to derive $c(\omega)$ let's take $\delta(S_0) = \delta_0$ and choose $P(\delta_0, S_0) = \delta_D(\delta_0)$ as an initial condition. This follows quite naturally from the fact that the probability of a transition between δ_0 and a certain δ during a step $\Delta_S = S - S_0$ is null at the very beginning, except for $\delta = \delta_0$, $S = S_0$, which means applying an Identity. The application of such an initial condition results in

$$c(\omega) = \frac{2}{\pi}\, \sin(\omega\gamma_0)\, e^{\frac{\omega^2}{2}S_0} \quad , \tag{61}$$

where $\gamma_0 = \delta_c - \delta_0$. In the end, the function $P(\gamma, S)$ can be derived by substituting $c(\omega)$ in equation (16) and integrating, so that

$$P(\gamma, S) = \frac{2}{\pi} \int_0^\infty \sin(\omega\gamma_0)\, \sin(\omega\gamma)\, e^{-\frac{S-S_0}{2}\omega^2}\, \mathrm{d}\omega \quad . \tag{62}$$

In order to solve the integral note that:

- by applying the Werner's formula for a product of sines

$$\sin(\omega\gamma_0)\, \sin(\omega\gamma) = \frac{1}{2}(\cos(\omega\Delta\delta) - \cos[2(\delta_c - \delta_0) - \Delta\delta]) \quad ; \tag{63}$$

- the integral can be split in two parts thanks to its additive linearity and both the resulting integral are therefore Fourier transforms of even Gaussian functions;

- according to the scaling relation of the Fourier transform

$$\mathcal{F}(e^{-\frac{\Delta S}{2}\omega^2}) = \frac{1}{\Delta S}\, e^{-\frac{(\Delta\delta)^2}{2\Delta S}} \quad , \tag{64}$$

  where $\Delta S = S - S_0$.

In the end, by taking into account all these facts together with the normalization of the Gaussian functions, I get the following solution:

$$P(\delta, S) = \frac{1}{\sqrt{2\pi\,\Delta S}}(e^{-\frac{(\Delta\delta)^2}{2\Delta S}} - e^{-\frac{[2(\delta_c-\delta_0)-\Delta\delta]^2}{2\Delta S}}) \quad . \tag{65}$$

As I anticipated above, I've so far derived the probability that the contrast density δ didn't cross the threshold before or just at the scale S.
What I'm really interested in is the fraction of trajectories exceeding the threshold prior to the scale S, which can be derived as the complement of the distribution $P(\delta, S)$:

$$F(S) = 1 - \int_{-\infty}^{\delta_c} P(\delta, S)\,\mathrm{d}\delta = \mathrm{erfc}\left(\frac{\delta_c - \delta_0}{\sqrt{2}\,\Delta S}\right) \quad , \tag{66}$$

where one must make sure that the integral doesn't diverge in $-\infty$. This is why the first boundary condition is necessary. Equation (66) is well-argued because

$$\frac{1}{\sqrt{2\pi\,\Delta S}} \int_{-\infty}^{\delta_c} e^{-\frac{(\Delta\delta)^2}{2\,\Delta S}}\,\mathrm{d}\delta = -\frac{1}{\sqrt{2\pi\,\Delta S}} \int_{-\infty}^{\delta_c} e^{-\frac{[2(\delta_c-\delta_0)-\Delta\delta]^2}{2\,\Delta S}}\,\mathrm{d}\delta = \frac{1}{2}\mathrm{erf}\left(\frac{\delta_c - \delta_0}{\sqrt{2}\,\Delta S}\right) \tag{67}$$

Indeed, the arguments of the exponential functions becomes equal when $\delta = \delta_c$. Take now $\delta_0 = 0$ and $S_0 = 0$, meaning an arbitrary starting value at a very large scale, and remember that $S = \sigma^2$. By doing that, I get exactly the result of the Press-Schechter formalism without being necessary to add a heuristic factor of 2. This follows as a consequence of the second exponential term in equation (65), which takes into account all the trajectories that crossed the barrier at a scale smaller than S (larger R, or M) and which could subsequently have crossed again the threshold downwards, meaning an underdense region at a larger S (smaller R). In other words, it solves the cloud-in-cloud problem in a formal way.
Hence, let's derive the Mass Function. First of all, a proper definition of the differential probability distribution $\mathrm{d}F/\mathrm{d}S$ of the first up-crossing is needed. Given a generic initial datum (δ_0, S_0), it can be computed as

$$f(S|\delta_0, S_0) = \frac{\mathrm{d}F(S)}{\mathrm{d}S} = -\frac{\mathrm{d}}{\mathrm{d}S}\int_{-\infty}^{\delta_c} P(\delta, S)\,\mathrm{d}\delta = \frac{\delta_c - \delta_0}{\sqrt{2\pi}\,\Delta S^{3/2}}\, e^{\frac{(\delta_c-\delta_0)^2}{2\,\Delta S}} \quad . \tag{68}$$

Note that $f \geq 0\ \forall S$. Then:

$$\frac{\mathrm{d}F}{\mathrm{d}M} = \frac{\mathrm{d}F}{\mathrm{d}S}\left|\frac{\mathrm{d}S}{\mathrm{d}M}\right| = \frac{1}{\sqrt{2\pi\,S}}\,\frac{\delta_c}{S}\left|\frac{\mathrm{d}S}{\mathrm{d}M}\right| e^{-\frac{\delta_c^2}{2S}} \quad . \tag{69}$$

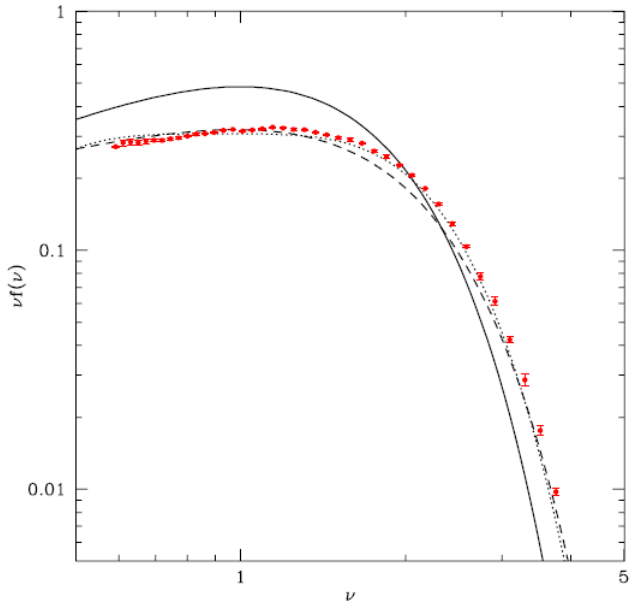

Figure 2: This plot features different curves representing the mass fraction in collapsed objects per logarithmic interval $\nu f(\nu)$. The solid line shows the predictions of the discussed Excursion Set model. The dashed and dotted lines represent fits by Sheth&Tormen(1999) and Jenkins et al.(2001). The red points consist in numerical data from N-body simulations by J.L. Tinker

In the end, the Mass Function follows from calculations similar to those of equation (49) and by setting $S = \sigma^2$:

$$\Phi(M) = \frac{\mathrm{d}n}{\mathrm{d}M} = \sqrt{\frac{2}{\pi}}\,\frac{\rho_M}{M^2}\,\frac{\delta_c}{\sigma}\left|\frac{\mathrm{d}\ln\sigma}{\mathrm{d}\ln M}\right| e^{-\frac{\delta_c^2}{2\sigma^2}} = \sqrt{\frac{2}{\pi}}\,\frac{\rho_M}{M^2}\,\nu\frac{\mathrm{d}\ln\nu}{\mathrm{d}\ln M}\,e^{-\frac{\nu^2}{2}} \quad , \tag{70}$$

which is the Press-Schechter Mass Function without any additional factor of 2.

Although this method provides a simple but effective expression for the Mass Function predicting rather accurately the overall features of the mass spectrum, it shows some limitations. This approach tends indeed to predict too many low-mass halos and too few high-mass halos. This fact is clearly shown in Figure 2, which features the mass fraction in collapsed objects $\nu f(\nu) = \mathrm{d}F/\mathrm{d}\ln\nu$ per logarithmic interval in ν.

An example by Zentner(2006) of $\delta(S)$ random walks with independent S step is shown in Figure 3. This is what I'm trying to reproduce in the following Chapter.

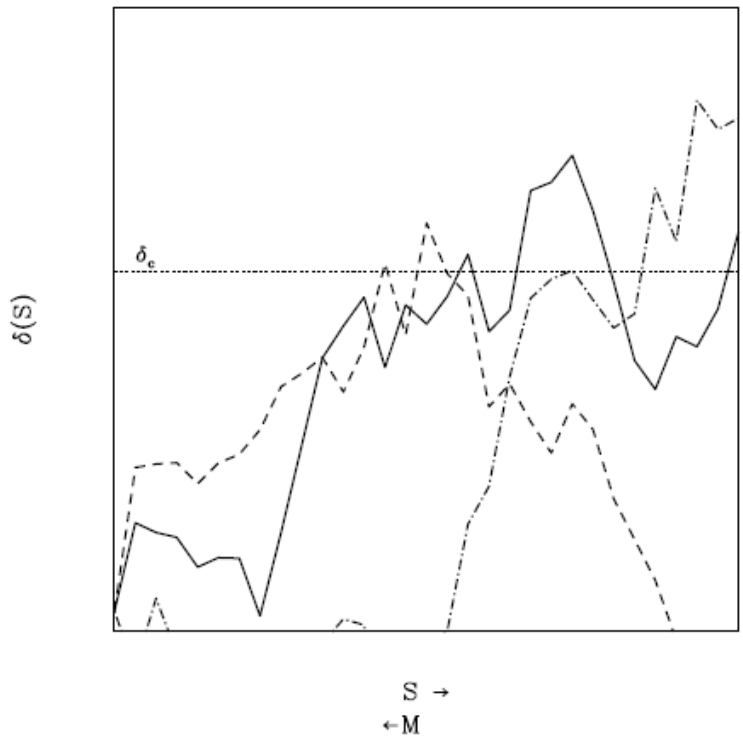

Figure 3: This plot features three examples of $\delta(S)$ random walks with independent S step, with arbitrary axes. The second exponential term in equation (65) provides an analytical argument for the fact that the trajectories can cross the threshold many times both upwards and downwards. From Zentner(2006)

4

NUMERICAL APPLICATIONS OF THE EXCURSION SET

In this Chapter I carry out a numerical application of the Excursion Set theory in its simplest approach of independent steps, disclosed in the previous Chapter. What I do is building a Montecarlo simulation and trying to extract the Mass Function from that.
As expressed in the previous Chapter, the choice of a k-space top-hat filter function makes the steps in S independent on each other. Hence, the probability of a transition $\Delta\delta$ is Gaussian with zero mean and variance $\sigma = \Delta S$, regardless of the starting scale.
The starting point of the simulation is therefore building a proper random walk and seeing at which S the contrast density δ crosses the threshold δ_c. Then:

- several random walks are generated by repeating the same procedure many times;
- the S-values at which the barrier is passed are recorded and turned into $\nu = \delta_c/\sqrt{S}$;
- I choose proper bins and plot a histogram featuring how many times the random walk crosses δ_c within the interval $\Delta\nu$ of a certain bin;
- the columns of the histogram are fitted with a proper function;
- I compute the function $f(\nu)$ by derivating the fitting function in respect with ν.

In the end, several simulations are put together in order to find an average result, equipped with proper error bars.

1 GENERATION OF GAUSSIAN RANDOM FIELDS AND THE BUILDING OF A RANDOM WALK

I anticipated above that the basic idea is developing a random walk with the above-mentioned features. In order to do that, I started by generating

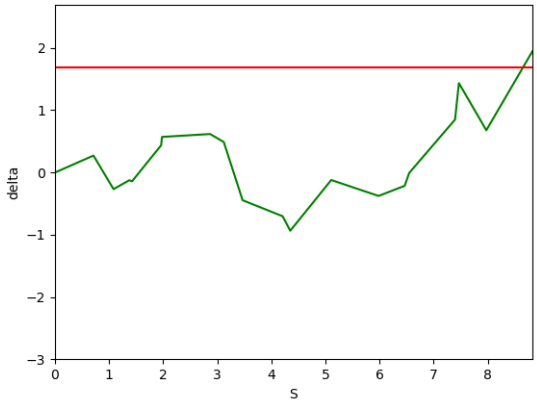

Figure 4: This plot shows a single random walk in δ. At each step ΔS in S the random walk is shifted to the right of ΔS. Note that the trajectory can pierce the barrier many times, both upwards and downwards. The threshold is displayed as a red horizontal line

random numbers uniformly in the interval $[0, 1)$. These numbers represent the indepedent steps in S. Then, for each S-step I produced a step in δ by generating a random number with a Gaussian distribution having $\sigma^2 = S$, as requested by the k-space top-hat filter. In this way the generation of Gaussian random fields allowed me to achieve the desired random walk in δ. Examples of outcome of this procedure are displayed in Figures 4 and 5. Note that this is exactly the result showed in Figure 3 in the previous Chapter.

2 THE MONTECARLO SIMULATION

The simulation I did is based on the repetition of the above-mentioned procedure many times, that is, thousands times. Let n be the number of repetitions. The algorithm works as I anticipated in the introductory part of this Chapter. Every single random walk goes on until it reaches the threshold value $\delta_c = 1.686$ for the first time. When it happens, the S-value of crossing is registered in a proper list and this procedure is repeated n times. Then, I converted the set of S-values into a set of ν-values by computing $\nu = \delta_c / \sqrt{S}$ for each S. In the end, I built a histogram featuring the ν-values in the x-axis and their occurrence in the y-axis. For each column I derived a data-point of coordinates $(\overline{\nu}, N)$, where $\overline{\nu}$ is the mean value between the two limits in ν of each bin and N is the height of the column. This histogram is showed with normalized columns independently on the number of random

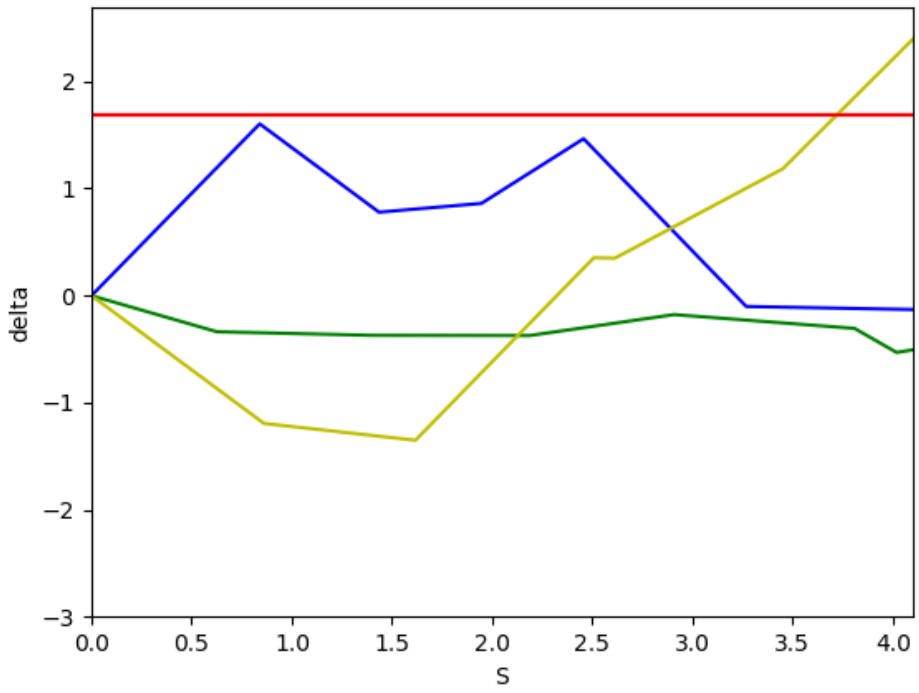

Figure 5: This plot features three examples of δ random walks with independent S step, like the previous plot. The threshold is displayed as a red horizontal line

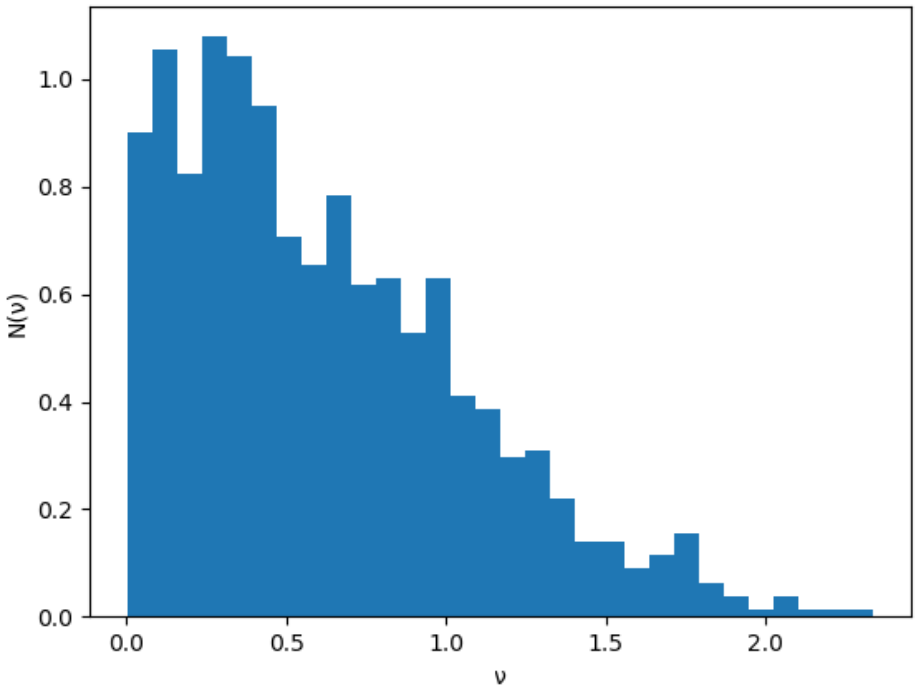

Figure 6: This histogram shows the occurrence of the ν-values in a 1000 random walks simulation

walks, so that simulations consisting of a different number of random walks can be compared. An example of such a histogram is featured in Figure 6, corresponding to a simulation with 1000 random walks. What this kind of histogram tells us is the number (or the number density, if normalized) of times the threshold is exceeded in a certain bin. As I'm interested in gaining the Mass Function from this simulation, I'll proceed as follows. As described in the previous Chapter, the function

$$\nu f(\nu) = \frac{\mathrm{d}N}{\mathrm{d}\ln\nu} = \sqrt{\frac{2}{\pi}}\,\nu\, e^{-\frac{\nu^2}{2}} \tag{71}$$

indicates the mass fraction of collapsed objects per logarithmic interval in ν. This means that, if I knew the primitive of the function $f(\nu)$ and it was a good fitting function for the data-points I got from the histogram, then the Mass Function would be recovered.

Let us remember that the Gaussian function doesn't have an explicit analy-

tical primitive, that is, it can only be expressed as an integral. Indeed, the complementary error function is expressed as

$$\operatorname{erfc}\left(\frac{\delta}{\sqrt{2\,S}}\right) = \int_{\delta_c}^{\infty} e^{\frac{\delta^2}{2S}}\,\mathrm{d}x \quad , \tag{72}$$

and its derivative $f(\delta)$ in respect with δ is just

$$f(\delta) = -e^{-\frac{\delta^2}{2S}}\Big|_{\delta_c}^{\infty} = e^{-\frac{\delta_c^2}{2S}} = e^{-\frac{\nu^2}{2}} \quad , \tag{73}$$

except for the normalization factor. In other words, I'll try and see whether the erfc is a good fitting function or not, since its graphic is known, even though it is an integral function. Figures 7 and 8 show two examples of fit with the erfc function. They represent respectively a 1500 and a 2500 random walks simulation. By looking at these two fits it turns out that the aforementioned function produces if not a good a fit, at least a reasonable one.

3 ESTABLISHING THE FIT'S GOODNESS

Even though the fit looks appropriate, a stronger proof of its validity is needed. This can be achieved by repeating the up-to-now-described procedure many times, by computing a mean value of every column's height and by associating to the computed averages proper error bars. Figure 9 displays the fitted data-points with their errors bars. The error bars come from a set of 15 simulations, each of which includes 1000 random walks.

Note that the automatic binning of the software make the bins regarding different simulations not identical to each other, that is, their ν-limits are slightly different. Anyway, if I consider the mean points in ν of correspondent bins of different simulations, they all lay in the interval identified by the limits of the correspondent bin of one of the simulations, e.g. the first simulation. This means that, in order to make things faster and more simple, the binning of the first simulation can be employed for all the simulations. Even though this procedure isn't completely correct, it can be used as a good approximation. The error bars have been obtained by computing the standard deviation of each set of column heights values.

Moreover, it can easily noticed that the fore coefficient of the fitting function doesn't guarantee the exact normalization of the erfc, even though it is very

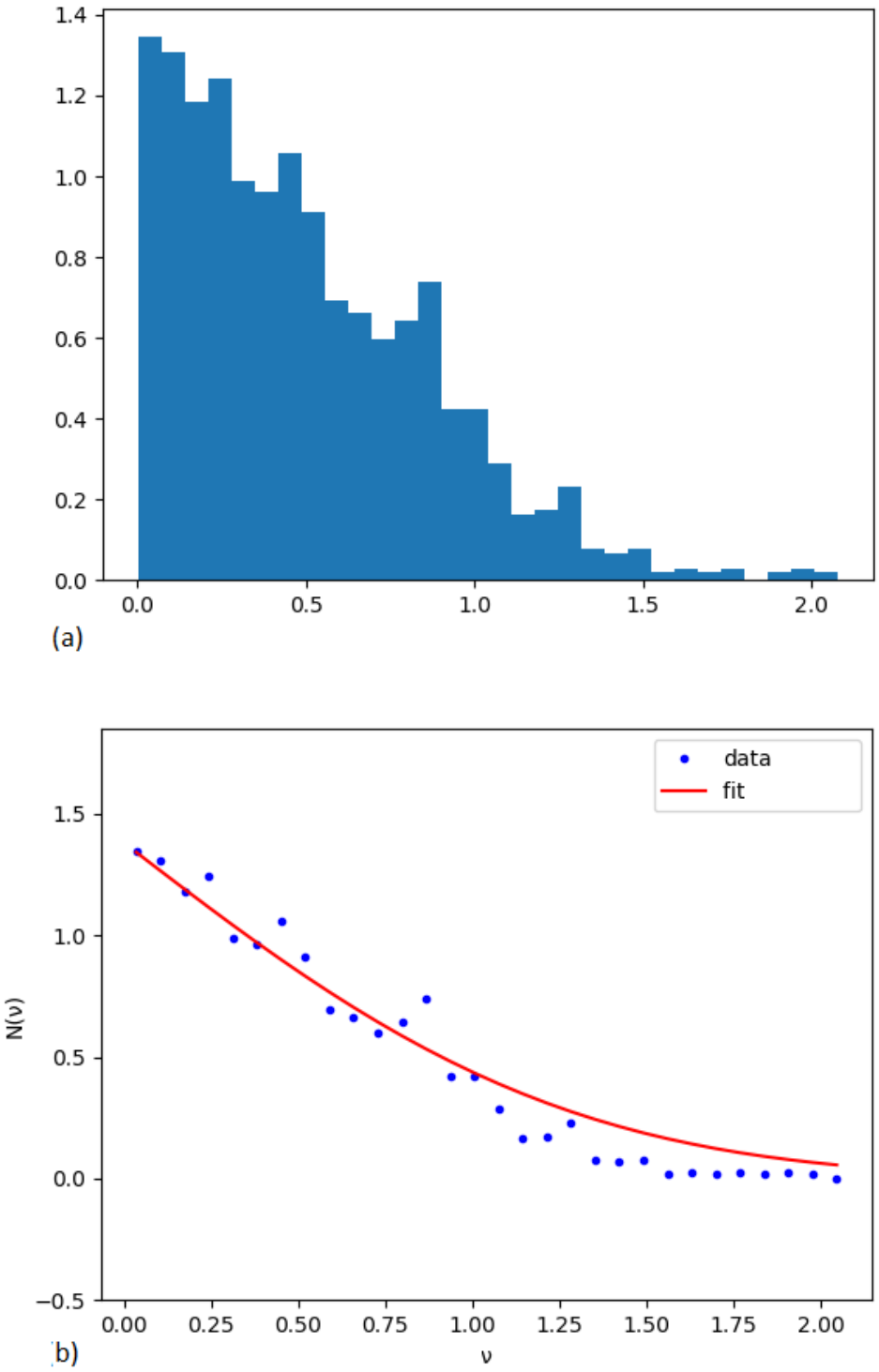

Figure 7: (a) Histogram of a 1500 random walks simulation; (b) the plot shows the data-points fitted by the erfc function, with a proper coefficient

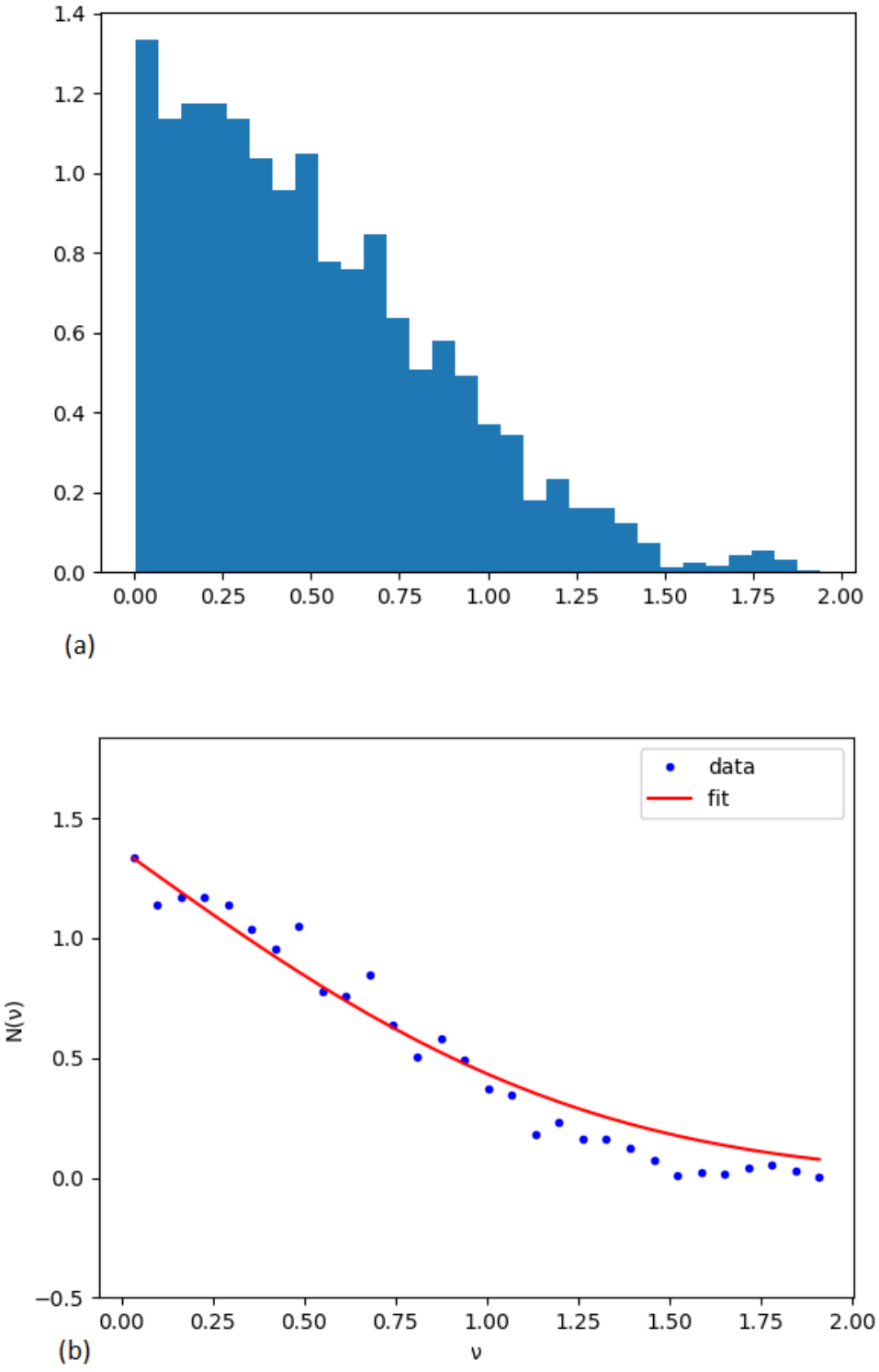

Figure 8: (a) Histogram of a 2500 random walks simulation; (b) the plot shows the data-points fitted by the erfc function, with a proper coefficient

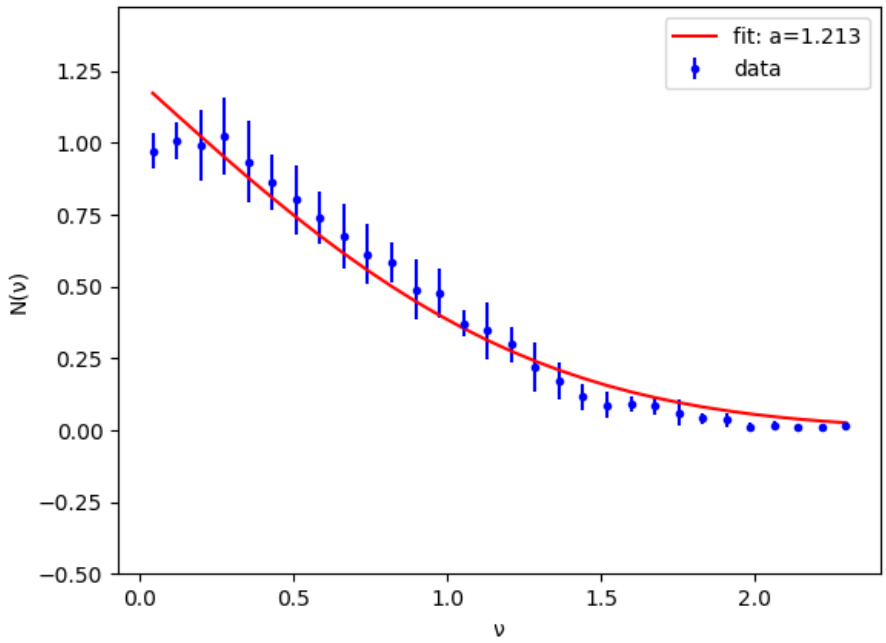

Figure 9: This plot shows the fitted data-points with their errors bars. The error bars come from a set of 10 simulations, each of which includes 1000 random walks

similar to what it should be. Indeed, my fit provides a coefficient $a = 1.213$, while the correct normalization would present a fore coefficient $a = 1.253$. This fact can be explained by considering that of course the fit could be improved by using more random walks for each simulation (this process requires a much more powerful computer than mine) and by increasing the number of simulations. In this way, perhaps I would be able to achieve a better correspondence between coefficients.

The main programs I wrote and used to carry out the simulations and to plot histograms and fits are reported in APPENDIX A.

5

RANDOM WALKS WITH DIFFERENT FILTERS

This ending Chapter allows us to take a look of how a contrast density random walk changes depending on which filter function one employes. In this Chapter I follow the implementation presented by Desjacques et al.(2018). The filters I'm going to use are the same discussed in Chapter 2:

- top-hat filter in the k-space;
- top-hat filter in the real space;
- Gaussian filter in the real space.

The goal of this Chapter is mainly discussing the numerical implementation of these filters in a random walk.
Let in what follows $Q(R)$ be a *stochastic force* defined as

$$Q(R) = \frac{\mathrm{d}\delta(R)}{\mathrm{d}R} \quad . \tag{74}$$

What this quantity tells us is the rate of change of the smoothed linear density $\delta(R)$. As we already know from the previous Chapters, $Q(R)$ has a null average value $\langle Q(R) \rangle = 0$ but has a non-zero two-point function given by

$$\langle Q(R_1)\, Q(R_2) \rangle = \frac{1}{2\pi^2} \int_k P(k)\, \frac{\mathrm{d}W_{R_1}(k)}{\mathrm{d}R_1} \frac{\mathrm{d}W^*_{R_2}(k)}{\mathrm{d}R_2} \tag{75}$$

1 THE SHARP-k FILTER

This is the case I already discussed in Chapter 3 with respect to the Press-Schechter formalism. A top-hat filter in the k-space makes the steps uncorrelated and the random walk fully Markovian. The choice of such a filter is very popular in literature as it allows to derive an exact solution to

the first-crossing problem.
The sharp-k filter is defined as

$$W(k, R) = \begin{cases} 1 & \text{if } k \leq 1/R \\ 0 & \text{if } k > 1/R \end{cases} = \Theta(1 - kR) \quad , \tag{76}$$

where Θ is the Heaviside step function, so that its derivative in respect of the scale R is

$$\frac{\mathrm{d}W_R(k)}{\mathrm{d}R} = \frac{\mathrm{d}\Theta(1 - kR)}{\mathrm{d}R} = -\frac{k}{R}\,\delta_D\left(k - \frac{1}{R}\right) \quad , \tag{77}$$

where δ_D indicates a Dirac's delta. By substituting this result in equation (75) , I get

$$\langle Q(R_1)\, Q(R_2)\rangle = -\frac{k^2\, P(k)}{2\pi^2}\bigg|_{k=1/R_1} \frac{1}{R_1^2}\,\delta_D(R_1 - R_2) \quad . \tag{78}$$

I achieved this result by:

- considering that the fore minus is due to the complex conjugate;
- considering the resulting Dirac's delta comes from the fact that $\delta_D(k - 1/R) = 0\,\forall k \neq 1/R$, and the product of the two deltas is equal only if $R_1 = R_2$;
- noticing that the evaluation in $k = 1/R_1$ and the factor of $1/R_1^2$ again are due to the previous consideration.

I rewrite now equations (74)-(78) in terms of $\ln k = -\ln R$ getting

$$\frac{\mathrm{d}\delta(R = 1/k)}{\mathrm{d}\ln k} = Q(\ln k) \quad \text{and} \tag{79}$$

$$\delta(R) = \int_{-\infty}^{-\ln R} \mathrm{d}\ln k'\, Q(\ln k') \quad . \tag{80}$$

The two-point function becomes therefore

$$\langle Q(\ln k_1)\, Q(\ln k_2)\rangle = \frac{k_1^3\, P(k_1)}{2\pi^2}\,\delta_D(\ln k_1 - \ln k_2) \quad . \tag{81}$$

Note now that both equations (79)-(81) don't depend explicitly on R, that is, the stochastic forces are uncorrelated. In other words, the δ-steps are

uncorrelated as we had expected. Furthermore we can change the initial conditions setting $(R_i, \delta(R_i)) = (\infty, 0)$, where the R_i is the initial scale. Under these circumstances I can get a numerical solution by discretizing the steps in the k-space, that is, by proceeding via subsequent $\Delta \ln k_i$. By doing that the stochastic force owns to a Gaussian distribution with zero mean and variance

$$\sigma_Q^2 = \frac{k_i \, P(k_i)}{2\pi^2 \, \Delta \ln k_i} \tag{82}$$

and the random walk can be achieved by computing $\delta(R)$ as the following sum:

$$\delta(R) = \sum_{k_i < 1/R} r_i \sqrt{\frac{k_i^3 \, P(k)}{2\pi^2} \, \Delta \ln k_i} \quad , \tag{83}$$

where r_i is a random number originating from a Gaussian distribution $\mathcal{N}(0, 1)$, that is, with zero mean and standard deviation $\sigma = 1$.

2 OTHER FILTERS: REAL TOP-HAT AND GAUSSIAN

The main point of the top-hat filter in the Fourier space is that the derivative of the window function is a Dirac's delta and this makes all the stochastic forces on different scales independent from each other, since they're not vanishing only at the scale they're centered on. This fact is not true for all other filters whose derivative with respect to the scale R is not a δ_D. This means basically that every stochastic force $Q(R_i)$ depends on all the previous steps $[Q(R_0), Q(R_1), \ldots, Q(R_{i-1})]$ and this makes of course the contrast density random walk non-Markovian.
I want now to build such a random walk with a generic filter. The starting point is considering that $\delta(\mathbf{k})$ is Gaussian. This implies that the Fourier amplitudes of different wavenumbers k are independent on each other. Let us then start by writing the smoothed linear density field in k-coordinates as

$$\delta(R) = \int_{\mathbf{k}} \mathrm{d}\mathbf{k}^3 \, \delta(\mathbf{k}) \, W_R(k) \quad . \tag{84}$$

Let now $Q^{sk}(\mathbf{k})$ be the stochastic force in the k-space for the sharp-k filter. By looking at this last expression and at equation (80), it turns out clearly that $Q^{sk}(\mathbf{k})$ is nothing but $\delta(\mathbf{k})$ integrated over a spherical shell in Fourier

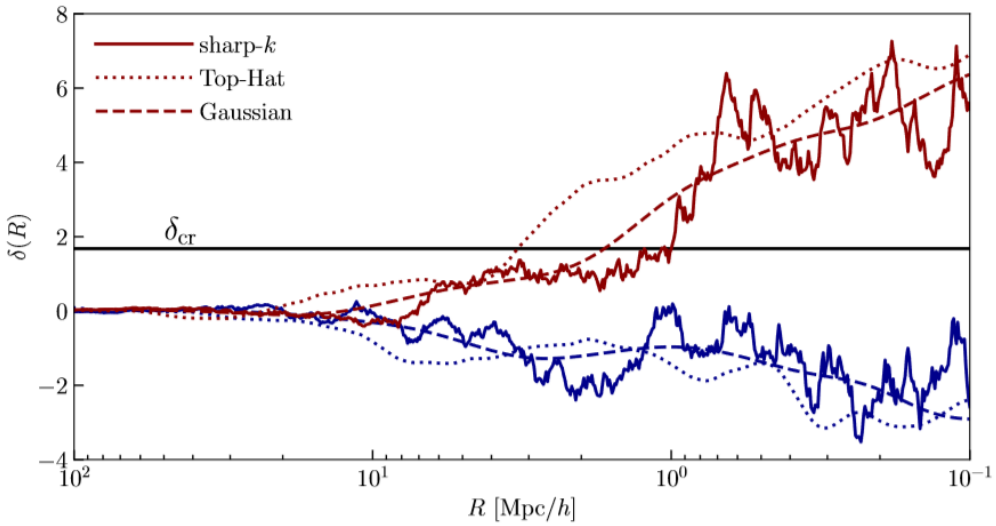

Figure 10: This plot shows the three discussed random walks. The solid lines show the sharp-k random walks, the dashed lines those obtained with the Gaussian filter and the dotted lines feature the real top-hat ones. Notice that the Gaussian and real top-hat appear smoother than the sharp-k ones. From Desjacques et al.(2018)

space with fixed logarithmic width $\mathrm{d}\ln k$. According to this fact, the contrast density can be written in terms of $Q^{sk}(\mathbf{k})$ and the filter $W_R(k)$ as

$$\delta(R) = \int_0^\infty \mathrm{d}\ln k' \, Q^{sk}(\ln k') \, W_R(\ln k) \quad , \tag{85}$$

where the integration runs from 0 to ∞.
The numerical implementation follows then by exploiting the stochastic force for sharp-k filter $Q^{sk}(\ln k')$. In other words, the steps in the random walk can be obtained by simply multiplying the argument of the sum in equation (83) by the k-space window function $W_R(k)$. A comparison between the three different discussed random walks is showed in Figure 10, taken from Desjacques et al.(2018). Notice that, as the steps obtained with the real top-hat and Gaussian filters are correlated, then the resulting non-Markovian random walks appear much smoother than those built with the Fourier space top-hat filter.

3 COMPARISON BETWEEN ALGORITHMS

In this last section I make a comparison between the aforementioned algorithms and the code I developed.

My program is based on a simple generation of Gaussian random fields. According to Zentner(2007), the random walk starts by the variance value $S = 0$ and at each S-step ΔS a δ-step comes into being by generating a random number following a Gaussian distribution with zero mean and variance $\sigma^2 = \Delta S$. Then, the algorithm is set in the real space and plots a x-axis in S. On one hand, this code is quite concise and relatively easy to build. Furthermore, the results are quite fine and it doesn't need any assumptions on the power spectrum. On the other hand, the disadvantages are mainly that this algorithm can be applied only to the sharp-k case, as it is the only filter that makes the steps uncorrelated. As a result, if one would build a random walk employing another filter function, then this code is not useful anymore. The algorithm proposed by Desjacques et al.(2018) rests on more solid theoretical basis. It takes place in the Fourier space and computes how the $\delta(R)$ random walk behaves by discretizing the k-steps. The process requires in this case some further calculations and a choice of a proper power spectrum $P(k)$, the latter not being requested in my algorithm. Hence, upon these points this procedure appears unfavourable. However, as I discussed above such a code allows to implement every kind of filters by simply multiplying its Fourier-space form by the Fourier top-hat filter. Moreover, the plot shows R instead of S in the x-axis and this makes by construction the δ-steps larger and larger while proceeding towards smaller scales. This reflects the presence of a power spectrum weighing differently the contribute of the wavenumber k at different scales. As far as the results are concerned, I carried out a set of simulations using only my algorithm, so that I cannot actually compare my results with any others.

6

APPENDIX A

In this final section I include some of the source codes I used to carry out the simulations:

- generation of a simple δ random walk with a *while* cycle:

```
import numpy as np
import matplotlib.pyplot as plt
def randomwalk(t):
    deltalist=[]
    slist=[]
    deltao=0
    so=0
    deltalist.append(deltao)
    slist.append(so)
    while deltalist[-1]<t:
            deltas=np.random.random()
            deltadelta=np.random.normal(0, deltas)
            s2=slist[-1] + deltas
            slist.append(s2)
            delta2=deltalist[-1] + deltadelta
            deltalist.append(delta2)
    print("slist", slist)
    print("deltalist", deltalist)
    plt.xlim([0,slist[-1]])
    plt.ylim([-3,t+1])
    plt.plot(slist,deltalist,"-g",
     label="Contrast density random walk")
    lineart=1.686
    plt.plot([0,slist[-1]], [lineart,lineart], "-r")
    plt.xlabel("S")
    plt.ylabel('delta')
    plt.show()
```

- Montecarlo simulation with m random walks. When the function is called with proper parameters, it returns a histogram featuring ν on the x-axis and the number density $N(\nu)$ in the y-axis. Moreover, it returns the bins' limits and the heights of the columns:

```
import numpy as np
import matplotlib.pyplot as plt

def simulation(m, threshold):
  s_final_list=[]
  nu_list=[]
  for i in range(m):
        deltalist=[]
        slist=[]
        deltao=0
        so=0
        deltalist.append(deltao)
        slist.append(so)

        while deltalist[-1]<threshold:
          ddeltas=np.random.random()
          deltas=np.sqrt(ddeltas)
          deltadelta=np.random.normal(0, deltas)
          s2=slist[-1] + ddeltas
          slist.append(s2)
          delta2=deltalist[-1] + deltadelta
          deltalist.append(delta2)

  s_final_list.append(slist[-1])
 nu=threshold/np.sqrt((slist[-1]))
 nu_list.append(nu)
 print("(1) s_final_list")
 print(s_final_list)
 x=np.array(nu_list)
 n, bins, patches= plt.hist(x, bins=30, density=True,
  histtype='stepfilled', log=False)
 plt.xlabel('nu')
 plt.ylabel('N(nu)')
```

```
    plt.show()
    print("————————————————————————————————————————————")
    print("(2) column_values")
    print("(3) bins_values")
    return(n, bins)
```

- this program imports the bins' limits and the column's heights obtained from the previous code, computes the mean point of each bin's interval, build a point for each bin (see CHAPTER 4) and fits the datapoints with a erfc function. In the version I report below, it takes up several sets of values got by different simulations and use them to plot the error bars:

```
import numpy as np
import matplotlib.pyplot as plt
from scipy.special import erfc
from scipy.optimize import curve_fit
from scipy.integrate import quad

def errors(m):
  dat = np.genfromtxt('val_bins_pimp.txt')
  bins=dat[m,:]
  k=len(bins)
  values_list=[]
  errbar_list=[]
  for s in range(k):
        val_list=[]
        for t in range(m):
          val=dat[t,s]
          val_list.append(val)
          val_array=np.array(val_list)
    mean=np.mean(val_array)
    std=np.std(val_array)
    values_list.append(mean)
    errbar_list.append(std)

xdatalist=[]
for i in range(k-1):
```

```
    x=(bins[i+1]+bins[i])/2
    xdatalist.append(x)

    zero=values_list[-1]
    values_list.remove(zero)
    xdata=np.array(xdatalist)
    ydata=np.array(values_list)

    zero_err=errbar_list[-1]
    errbar_list.remove(zero_err)
    err_array=np.array(errbar_list)
    print('*x_data: ',xdatalist)
    print('*y_data: ',values_list)
    print('*err_array: ',errbar_list)


def func(x, a):
    return a*erfc(x/np.sqrt(2))
plt.errorbar(xdata,ydata,yerr=err_array,
    fmt='b.', label='data')
popt, pcov = curve_fit(func, xdata, ydata)
plt.plot(xdata, func(xdata, *popt),
    'r-',label='fit: a=%5.3f'% tuple(popt))
plt.xlabel('nu')
plt.ylabel('N(nu)')
plt.ylim([-0.5, ydata[0]+0.5])
plt.legend()
plt.show()
```

BIBLIOGRAPHY

[1] Desjacques V. et al., *Large-Scale Galaxy Bias*, Baltimore, Physics Reports, Volume 733, 2018

[2] Franceschini A., *Corso di Cosmologia. Laurea triennale in Astronomia*, Padova, 2013

[3] Liddle A., *An Introduction to Modern Cosmology*, Chichester, John Wiley & Sons Ltd, 2003

[4] Tormen G., *Formazione delle strutture cosmiche*, Padova, 2012

[5] Zentner A.R., *The Excursion Set Theory of Halo Mass Functions, Halo Clustering, and Halo Growth*, Chicago, IJMPD, Volume 16, Issue 05, pp.763-815, 2007